Process and signature of initiation on a finite fault system: a spectral approach

Christophe Voisin,[1,]* Michel Campillo,[1] Ioan Ionescu,[2] Riad Hassani[3] and Quoc-Lan Nguyen[4]

[1] *Laboratoire de Géophysique Interne, Observatoire de Grenoble, Université Joseph Fourier,* BP 53X, 38041 *Grenoble Cedex, France.*
E-mail: cvoisin@moho.sdsu.edu
[2] *Laboratoire de Mathématiques Appliquées, Université de Savoie,* 73376 *Le Bouget de Lac, France*
[3] *Laboratoire d'Instrumentation Géophysique, Observatoire de Grenoble, Université de Savoie,* 73376 *Le Bouget de Lac, France*
[4] *Polytechnic Institut, Ho-Shi-Minh, Vietnam*

SUMMARY

We present a numerical approach, based on a spectral analysis, for the initiation of the unstable slip on a finite fault region. First we focus on one fault model. We study the relationship between the weakening parameter and the largest positive eigenvalue of the dynamic spectral problem. Since the numerical approach based on the integral equations proposed by Dascalu *et al.* (2000) is appropriate only for small eigenvalues we use a finite element method which permits accurate computations for large eigenvalues. We show the relation between fault length and the first eigenvalue that governs the duration of initiation duration. The value of the weakening rate can be evaluated from the strain field in the elastic medium over a domain of confidence. A specific pattern of deformation represents the signature of the initiation phase. The spectral analysis and the numerical methods used for the single fault model remain valid for more complex fault systems. The interaction between two faults is examined. Finally, we introduce the concept of spectral equivalence between a heterogeneous fault system and a homogeneous fault with renormalized friction law.

Key words: initiation, fault system, spectral analysis.

1 INTRODUCTION

Earthquake prediction is actually the Holy Grail of seismologists and the existence of precursory deformation is a big issue. Laboratory experiments on friction (Dieterich 1979; Ohnaka *et al.* 1987; Ohnaka & Kuwahara 1990) point out the existence of a phase of slow motion that precedes the propagation phase, leading to the rupture. They pointed out that this preseismic slip should be recognized as a manifestation of the initiation process preceding the dynamic rupture. Throughout this paper, we will refer to this phase as the rupture initiation or initiation. Ohnaka *et al.* (1987) showed through high resolution friction experiments, the relevance of the slip dependent friction law in the initiation process. They showed the existence of a characteristic length scale L_c, the critical slip. The shear stress degrades from the initial state τ_i to a residual dynamic level of friction τ_d with the ongoing slip. They also demonstrated the existence of

a nucleation zone over which the nucleation process occurs. The length of this zone can be related to the constitutive parameters of the friction law.

On the basis of these experiments, Campillo & Ionescu (1997) studied the initiation phase (Ida 1972) of an unstable antiplane shear process on an infinite fault under linear slip-weakening friction. They gave an analytical expression of the slip, derived from an eigenvalue analysis. Considering only the part of the displacement associated with positive eigenvalues, they defined the dominant part $w_d(t, x, y)$ as follows:

$$
\begin{aligned}
w_d(t, x, y) = \frac{\alpha}{\pi} \exp(-\alpha y) \int_{-\alpha}^{\alpha} \int_0^{+\infty} \int_{-\infty}^{+\infty} \exp[-\alpha s + i\xi(x - u)] \\
\times \left[\cosh\left(ct\sqrt{\alpha^2 - \xi^2}\right) w_0(u, s) \right. \\
\left. + \frac{1}{c\sqrt{\alpha^2 - \xi^2}} \sinh\left(ct\sqrt{\alpha^2 - \xi^2}\right) w_1(u, s) \right] du\, ds\, d\xi
\end{aligned}
$$

(1)

* Now at: Dept. of Geological Sciences, San Diego State University, 5500 Campanile Drive, San Diego, CA 92182-1020

where α is the weakening rate on the fault ($y=0$) divided by the rigidity, $w_0(x, y)$ and $w_1(x, y)$ the initial perturbation in displacement and velocity respectively. α is given by the following relation:

$$\alpha = \frac{(\mu_s - \mu_d)S}{GL_c} \qquad (2)$$

where G, L_c, μ_s, μ_d and S are respectively the rigidity modulus, the critical slip, the static friction coefficient, the dynamic friction coefficient and the normal stress. Eq. (1) shows that $w_d(t, x, y)$ is characterized by an exponential growth with time and a simple exponential dependence of the slip distribution with respect to the coordinate perpendicular to the fault. In response to a small perturbation (w_0, w_1) the instability will develop in a limited spectral domain. The limiting wavenumber is a function of the friction law and the elastic properties. The dominant part gives an accurate description of initiation. This is illustrated by the numerical comparison performed by Campillo & Ionescu (1997). They demonstrated that the dominant part is indistinguishable from the complete solution, except in the very beginning of initiation, when the slip is of the order of the perturbation and therefore negligible with respect to the final amplitude of the solution. The expression of the dominant part associated with positive real eigenvalues is obviously non-causal, as remarked by Knopoff *et al.* (2000). Indeed, since all the propagative terms are omitted, the dominant part is not expected to be causal. During the initiation the dominant part grows exponentially with time, while the propagative terms scale with the perturbation. This means that the mismatch between the full solution and the dominant part at the causality limit also scales with the initial perturbation. In the context of earthquake study, we suspect the early triggering event to be small and in practice undetectable. For this reason violation of causality in eq. (1), that is not a mathematical problem, is not important from a physical point of view either, since the measurable slip evolution is almost perfectly described by the dominant part.

The slip during the initiation phase starts very slowly and gradually increases with time. The transition from the initiation phase to the propagation phase occurs at the point on the fault which has slipped by L_c, the critical slip. At this time the crack front begins to propagate along on the fault. The duration of the initiation phase is approximated by:

$$T_c = \frac{b}{c} + \frac{1}{c\alpha} \ln \frac{\pi L_c}{2l(W_0 + W_1/c)} \qquad (3)$$

where l is the half width of the perturbation, b its distance to the fault, c the S wave velocity, W_0 and W_1 the weighted average of the initial perturbation (Campillo & Ionescu 1997). During initiation the slip grows on a zone whose characteristic length is given by:

$$l_c = \frac{\pi GL_c}{(\mu_s - \mu_d)S} \qquad (4)$$

Note that l_c is the only characteristic length scale associated with the infinite fault model. Dascalu *et al.* (2000) studied the initiation process on a 2-D finite fault of length $2a$. They introduced a non-dimensional parameter $\beta = a.\alpha$, and performed a stability analysis to determine a universal constant β_0 that depends only on the geometry of the antiplane problem. This

constant was found as:

$$\beta_0 \approx 1.15777388, \qquad (5)$$

and defines quantitatively the limit between stable ($\beta < \beta_0$) and unstable ($\beta > \beta_0$) behaviour of the fault. For a given weakening rate on the fault, the minimum length for an unstable behaviour is:

$$2a_c = \frac{\beta_0}{\alpha} = \frac{\beta_0 GL_c}{(\mu_s - \mu_d)S}. \qquad (6)$$

The critical fault length $2a_c$ for unstable behaviour is a completely different concept from the critical crack length l_c, defined in the infinite fault context. As a consequence, when the fault length $2a$ is much larger than $2a_c$, the pertinent characteristic length scale is l_c. The 'free' initiation process, as it would develop on an infinite fault, provides a good description of what really happens on the finite fault. The finite fault effect arises when the fault length $2a \to 2a_c$. One can feel that this time, the 'free' initiation process (infinite problem) is unlikely to describe the real initiation process. The fault finiteness will have an effect on the initiation process. This effect was shown by Ionescu & Campillo (1999). The main effect is that the duration of initiation is greatly increased as the fault length $2a$ tends to $2a_c$. Indeed, as it follows from Dascalu *et al.* (2000), the duration of initiation is $T_c \approx \lambda_0^{-1}$, where λ_0^2 is the largest eigenvalue, and long initiation duration is expected when $\beta \to \beta_0$. The goal is to determine how strongly the initiation process is affected by the fault finiteness.

Since the numerical approach based on the integral equations proposed by Dascalu *et al.* (2000) works only for small eigenvalues (i.e. β close to β_0) we present here a numerical approach to the initiation of unstable slip on a 2D finite fault, based on a finite element method (FEM). We compute λ_0, the largest positive eigenvalue of the dynamic spectral problem, as a function of β for the finite fault model. We study the asymptotic behaviour when $\beta \to \infty$ to deduce the infinite fault model. We compute the associated eigenfunction $\Phi_0(x, y)$ and the following ratio:

$$\gamma = -\frac{\partial_y \Phi_0(x, y)}{\Phi_0(x, y)}, \qquad (7)$$

where ∂_y is the partial derivative with respect to the perpendicular coordinate. This ratio represents the information on the weakening parameter (Campillo *et al.* 2001). In the infinite case, this ratio exactly equals α everywhere in the elastic space. In the case of the finite fault zone, we point out the existence of an initiation pattern that develops in the elastic body. This pattern is associated with the unstable behaviour of the fault zone. Moreover, we show the existence of a domain over which γ is nearly constant. More precisely, in case of a single fault segment, this ratio equals the weakening rate α over a so called domain of confidence, whose size is an increasing function of α. Hence, the weakening parameter that is defined only on the fault can be estimated during the initiation phase outside of the fault, inside the bulk. This analysis remains valid for more complex fault systems. We first consider a system composed of two identical segments. We show that β_0 decreases as the distance between the two segments also decreases. This proves that fault segments may interact during the initiation process. Then, we consider a more complex fault system, composed of 11 identical fault segments, separated by rigid barriers. Each fault segment is characterized by the same weakening parameter

β_{local}. We show the existence of the initiation pattern associated with each of the segments (locally, the fault system is reduced to only one fault segment). We also point out the existence of a global initiation pattern that is associated with the unstable behaviour of the whole fault system. We compute the dynamic spectral problem and derive the largest eigenvalue of the heterogeneous system. With the help of the relation between λ_0 and β computed in the one fault model, we get the corresponding equivalent weakening parameter $\beta_{equivalent}$. A simple homogeneous fault with a weakening rate $\beta = \beta_{equivalent}$ will have the same largest eigenvalue λ_0, and therefore the same general average behaviour during the initiation.

The global initiation pattern associated with the unstable behaviour of the whole system is characterized by a wide domain over which the ratio $-\{[\partial_y\Phi_0(x, y)][\Phi_0(x, y)]\} = \beta_{equivalent}/a$. Locally, close to the fault, each individual fault segment has its own domain of confidence over which we can measure the local weakening rate. The interaction of all segments produces a global pattern of deformation at some distance from the fault system. This collective domain of confidence provides an estimation of $\beta_{equivalent}$. There is a complete spectral equivalence, in terms of the initiation process, between a complex fault system with $\beta = \beta_{local}$ and a simple homogeneous single fault model with $\beta = \beta_{equivalent}$.

2 SPECTRAL APPROACH OF RUPTURE INITIATION ON A FINITE FAULT

The method presented hereafter is basically the same for an infinite fault (Campillo & Ionescu 1997) or for a single finite fault (Dascalu *et al.* 2000). For convenience we give the principal steps of the spectral method in this section.

2.1 Problem statement

We consider the 2D antiplane shearing on a bounded fault region Γ_f included in the plane $y = 0$ in an homogeneous linear elastic space. The fault region can be composed of a set of simple faults on which the contact is described by a slip dependent friction law. We assume an antiplane configuration, that is the displacement field is 0 in directions Ox and Oy and that u_z does not depend on z. The displacement is therefore denoted simply by $w(t, x, y)$. The elastic medium has the shear rigidity G, the density ρ and the shear velocity $c = \sqrt{G/\rho}$. The nonvanishing shear stress components are $\sigma_{zx} = \tau_x^\infty + G\partial_x w(t, x, y)$ and $\sigma_{zy} = \tau_y^\infty + G\partial_y w(t, x, y)$, and the normal stress on the fault plane is $\sigma_{yy} = -S(S > 0)$. The equation of motion is

$$\frac{\partial^2 w}{\partial t^2}(t, x, y) = c^2 \nabla^2 w(t, x, y) \tag{8}$$

for $t > 0$ and (x, y) outside of the fault Γ_f. The boundary conditions on Γ_f are

$$\sigma_{zy}(t, x, 0+) = \sigma_{zy}(t, x, 0-), \quad x \in \Gamma_f, \tag{9}$$

$$\sigma_{zy}(t, x, 0) = \mu(\delta w(t, x))S \, \text{sign}\left(\frac{\partial \delta w}{\partial t}(t, x)\right), \quad x \in \Gamma_f, \tag{10}$$

if $\partial_t \delta w(t, x) \neq 0$ and

$$|\sigma_{zy}(t, x, 0)| \leq \mu(\delta w(t, x))S, \quad x \in \Gamma_f, \tag{11}$$

if $\partial_t \delta w(t, x) = 0$, where $\delta w(t, x) = 1/2[w(t, x, 0+) - w(t, x, 0-)]$ is the half of the relative slip and $\mu(\delta w)$ is the coefficient of friction on the fault region. The initial conditions are denoted by w_0 and w_1, that is,

$$w(0, x, y) = w_0(x, y), \quad \frac{\partial w}{\partial t}(0, x, y) = w_1(x, y). \tag{12}$$

Since it is our intention to study the evolution of the elastic system near an unstable equilibrium position, we shall suppose that $\tau_y^\infty = S\mu_s$, where $\mu_s = \mu(x, 0)$ is the static value of the friction coefficient on the fault. We note that taking w as a constant satisfies eqs (8)–(11); hence $w \equiv 0$ is a metastable equilibrium position, and w_0, w_1 may be considered as a small perturbation of the equilibrium. We shall assume that the friction law has the form of a piecewise linear function:

$$\mu(x, \delta w) = \mu_s - \frac{\mu_s - \mu_d}{L_c}\delta w \quad \delta w \leq L_c, \tag{13}$$

$$\mu(\delta w) = \mu_d \quad \delta w > L_c, \tag{14}$$

where μ_s and $\mu_d(\mu_s > \mu_d)$ are the static and dynamic friction coefficients, and L_c is the critical slip. Let us assume in the following that the slip δw and the slip rate $\partial_t \delta w$ are nonnegative. Bearing in mind that we deal with a fault plane and with the evolution of one initial pulse, we may (for symmetry reasons) put $w(t, x, y) = -w(t, x, -y)$, hence we consider only one half-space $y > 0$ in eqs (8) and (12). With these assumptions, eqs (9)–(11) become

$$w(t, x, 0) = 0, \quad \text{for} \quad x \notin \Gamma_f, \tag{15}$$

$$\frac{\partial w}{\partial y}(t, x, 0) = -\alpha w(t, x, 0+) \quad \text{if} \quad w(t, x, 0) \leq L_c, \quad \text{for} \quad x \in \Gamma_f, \tag{16}$$

$$\frac{\partial w}{\partial y}(t, x, 0) = -\alpha L_c \quad \text{if} \quad w(t, x, 0) > L_c, \quad \text{for} \quad x \in \Gamma_f, \tag{17}$$

where α is given by eq. (2). Since the initial perturbation (w_0, w_1) of the equilibrium state $w \equiv 0$, is small, we have $w(t, x, 0+) \leq L_c$ for $t \in [0, T_c]$ for all x, where T_c is a critical time for which the slip on the fault reaches the critical value L_c at least at one point, that is, $\sup_{x \in \Gamma_f} w(T_c, x, 0+) = L_c$. Hence for a first period $[0, T_c]$, called in what follows the initiation period, we deal with a linear initial and boundary value problem (8), (12) and (16).

2.2 The nondimensional problem and its spectral expansion

In order to obtain a non dimensional formulation let us introduce a the characteristic length i.e. we put

$$x_1 =: \frac{x}{a}, \quad x_2 =: \frac{y}{a}$$

and we introduce the following nondimensional constant

$$\beta = a\alpha = a\frac{(\mu_s - \mu_d)S}{GL_c}. \tag{18}$$

Let us use the same notation Γ_f for the fault region in these new coordinates (i.e. $x_1 \in \Gamma_f$ if $x \in \Gamma_f$). From eqs (8), (12) and (16)

we deduce

$$\frac{\partial^2 w}{\partial t^2}(t, x_1, x_2) = \frac{c^2}{a^2}\nabla^2 w(t, x_1, x_2) \tag{19}$$

$$w(t, x_1, 0) = 0, \quad \text{for} \quad x_1 \notin \Gamma_f, \tag{20}$$

$$\frac{\partial w}{\partial x_2}(t, x_1, 0) = -\beta w(t, x_1, 0), \quad \text{for} \quad x_1 \in \Gamma_f, \tag{21}$$

$$w(0, x_1, x_2) = w_0(x_1, x_2), \quad \frac{\partial w}{\partial t}(0, x_1, x_2) = w_1(x_1, x_2). \tag{22}$$

Let us consider the following eigenvalue problem connected to eqs (19)–(22): find $\Phi: R \times R_+ \to R$ and λ^2 such that $\int_{-\infty}^{+\infty}\int_0^{+\infty}\Phi^2(x_1, x_2)dx_1dx_2 = 1$ and

$$\nabla^2\Phi(x_1, x_2) = \lambda^2\Phi(x_1, x_2) \quad \text{for} \quad x_2 > 0, \tag{23}$$

$$\Phi(x_1, 0) = 0, \quad \text{for} \quad x_1 \notin \Gamma_f, \tag{24}$$

$$\frac{\partial}{\partial x_2}\Phi(x_1, 0) = -\beta\Phi(x_1, 0) \quad \text{for} \quad x_1 \in \Gamma_f. \tag{25}$$

Since we deal with a symmetric operator we have real-valued eigenvalues λ^2, i.e. λ is real or purely imaginary. This symmetry property is specific to the slip dependent friction law used here.

The solution of eqs (19)–(22) can be generically written (in its spectral expansion) as:

$$w = w^d + w^w,$$

where w^d is the 'dominant part' and w^w is the 'wave part', given by:

$$w^d(t, x_1, x_2)$$

$$= \sum_{n=0}^{N-1}\left[\cosh(c|\lambda_n|t/a)W_n^0 + a\frac{\sinh(c|\lambda_n|t/a)}{c|\lambda_n|}W_n^1\right]\Phi_n(x_1, x_2), \tag{26}$$

$$w^w(t, x_1, x_2)$$

$$= \sum_{n=N}^{\infty}\left[\cos(c|\lambda_n|t/a)W_n^0 + a\frac{\sin(c|\lambda_n|t/a)}{c|\lambda_n|}W_n^1\right]\Phi_n(x_1, x_2). \tag{27}$$

where (λ_n^2, Φ_n) are the associated eigenvalues and eigenfunctions of eqs (23)–(25), and

$$W_n^0 = \int_{-\infty}^{+\infty}\int_0^{+\infty}\Phi_n(x_1, x_2)w_0(x_1, x_2)dx_1dx_2, \tag{28}$$

$$W_n^1 = \int_{-\infty}^{+\infty}\int_0^{+\infty}\Phi_n(x_1, x_2)w_1(x_1, x_2)dx_1dx_2, \tag{29}$$

the projections of the initial data on the eigenfunctions. Let N be such that

$$\lambda_0^2 > \lambda_1^2 > \dots > \lambda_{N-1}^2 > 0 > \lambda_N^2 > \dots$$

The use of the expression of the dominant part w^d instead of w leads to a solution in which the perturbation is severely smoothed by the finite wavenumber integration. However, after a while, the propagative terms become negligible and the shape of the slip distribution is almost perfectly described by the dominant part.

2.3 Stability analysis; the static eigenproblem

One can easily remark that $w \equiv 0$ is a stable position if $\lambda_0^2 < 0$ (i.e. $N = 0$). In this case the dominant part w^d vanishes and the system has a stable behaviour. Hence it is important to obtain a condition on β, that determines the positiveness of the eigenvalues λ^2. Since β is nondimensional such a condition depends only on the geometry of Γ_f (number of fault segments) and completely characterizes the stability. In order to perform a stability analysis let us introduce the eigenvalue problem corresponding to the static case: find $\phi: R \times R_+ \to R$ and β such that $\int_{-\infty}^{+\infty}\int_0^{+\infty}\varphi^2(x_1, x_2)dx_1dx_2 = 1$ and

$$\nabla^2\varphi(x_1, x_2) = 0; \quad \text{for} \quad x_2 > 0, \tag{30}$$

$$\varphi(x_1, 0) = 0, \quad \text{for} \quad x_1 \notin \Gamma_f, \tag{31}$$

$$\partial_{x_2}\varphi(x_1, 0) = -\beta\varphi(x_1, 0) \quad \text{for} \quad x_1 \in \Gamma_f. \tag{32}$$

This problem has a sequence of positive eigenvalues $0 < \beta_0 < \beta_1 < \dots$ with $\lim_{n \to \infty}\beta_n = +\infty$. The eigenvalues β_k are closely related to those of the dynamic eigenvalue problem (23)–(25). Indeed, they correspond to the intersection points of the increasing curves $\beta \to \lambda_k^2(\beta)$ with the axis $\lambda^2 = 0$ (i.e. $\lambda_k^2(\beta_k) = 0$). The first eigenvalue β_0 has a major signification in the static stability analysis:

$$\text{if} \quad a\frac{(\mu_s - \mu_d)S}{GL_c} = \beta < \beta_0 \quad \text{then} \quad w \equiv 0 \quad \text{is stable}. \tag{33}$$

3 THE FINITE ELEMENT APPROACH

In order to use a FEM, the finite fault zone is embedded in a bounded elastic domain $\Omega =]-L, L[\times]0, L[$. The infinite elastic half space is limited by a fictitious boundary all over which the displacement is negligible. So that we impose a null displacement along Γ_d, the part of the boundary of Ω which is not on the fault Γ_f (see Fig. 1). Let us give first the variational formulation of (23)–(25) : find $\Phi: \Omega \to R$ and λ^2 such that $\Phi = 0$ on Γ_d and

$$\int_\Omega \nabla\Phi(x_1, x_2) \cdot \nabla v(x_1, x_2)dx_1dx_2 - \beta\int_{\Gamma_f}\Phi(x_1, 0)v(x_1, 0)dx_1$$

$$= -\lambda^2\int_\Omega \Phi(x_1, x_2)v(x_1, x_2)dx_1dx_2,$$

for all functions $v \in V_h$ (V_h is a finite element space of dimension N, composed of continuous and affine functions over each triangle) such that $v = 0$ on Γ_d. The domain Ω has a polygonal boundary $\Gamma_d \cup \Gamma_f$. Therefore it is possible to cover exactly Ω with triangles. Ω is meshed using Delaunay conditions. The size of the elements decreases as we get closer to Γ_f, where a strong variation of the stress is expected. Let $\{e_1, e_2, \dots, e_N\}$ be the canonical base of V_h and let us denote by

$$M_{ij} = \int_\Omega e_i(x_1, x_2)e_j(x_1, x_2)dx_1dx_2,$$

$$K_{ij} = \int_\Omega \nabla e_i(x_1, x_2) \cdot \nabla e_j(x_1, x_2)dx_1dx_2,$$

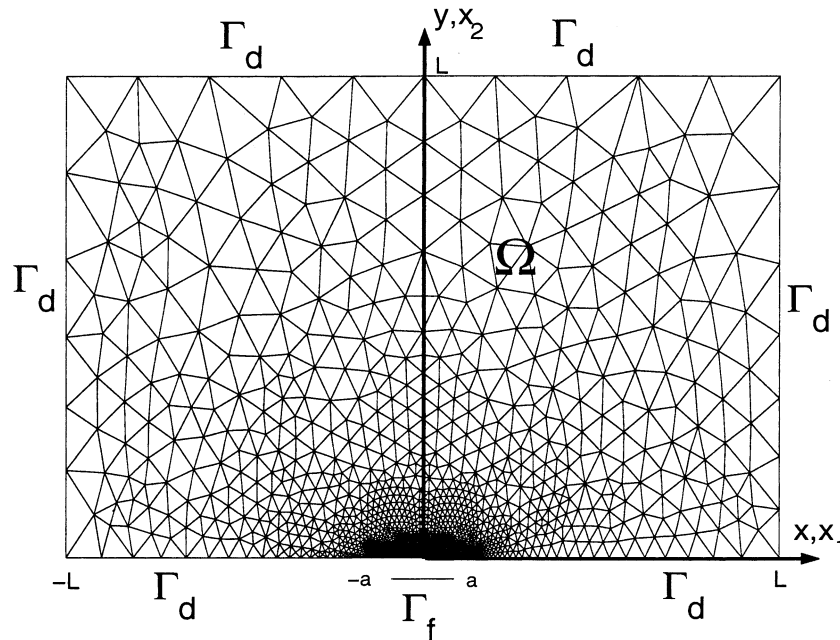$$B_{ij} = \int_{\Gamma_f}\alpha e_i(x_1, 0)e_j(x_1, 0)dx_1$$

Figure 1. Geometry of the problem. $\Gamma_f = [-a, a]$ is the frictional surface. Γ_d is the fictitious boundary. $\Omega = [-L, L] \times [0, L]$ is the elastic half space. x and y are the two coordinates. For symmetry reasons, we consider only $y > 0$ values. Ω is meshed with triangular elements using Delaunay conditions. Note the increase in the number of elements near the fault Γ_f.

mass, stiffness and boundary matrices. If we put

$$\Phi(x_1, x_2) = \sum_{i=1}^{N} F_i e_i(x_1, x_2), \quad \varphi(x_1, x_2) = \sum_{i=1}^{N} f_i e_i(x_1, x_2)$$

then the eigenvalue problems (23)–(25) and (30)–(32) can be written as :

$$(K - B)F = -\lambda^2 MF, \quad Kf = \beta Bf. \tag{34}$$

The stiffness matrix is factorized using a Cholevsky decomposition. The results are fed to a numerical solver based upon an Arnoldi-Lanczos algorithm that provides good approximations of the couples (λ_i^2, Φ_i). The positive eigenvalues contribute to the dominant part of the slip evolution. The largest one, λ_0^2, governs the essential of the slip evolution and controls the duration of the initiation phase.

4   THE CASE OF ONE HOMOGENEOUS FAULT

We consider the case of one homogeneous fault of length $2a$ embedded in an elastic half space $\Omega = [-L, L] \times [0, L]$, as shown in Fig. (1). We have chosen L large enough ($L = 10a$) to reduce the influence of the fictitious boundary conditions.

In order to verify the accuracy of the FEM we computed the static spectral problem. We compare the eigenvalues obtained by a FEM with 250 points on the fault with the results obtained by Dascalu *et al.* (2000) with a more accurate integral equation method with a finer grid of 1000 points along the fault. We find that the finite element method employed here provides

good approximations of the $\{\beta_i\}$. The resolution of this spectral problem by two independent numerical methods validates both of them.

Fig. (2) presents the normalized eigenfunction $\varphi_0(x, y)$ corresponding to β_0. The maximum amplitude is attained at the centre of the fault. Outside the fault ($y > 0$), the amplitude of φ_0 decays rapidly. The shape of φ_0 agrees with the unstable evolution of the slip velocity on the fault, as computed by a finite difference method.

4.1   Influence of the weakening parameter on the spectrum

For a finite fault of length $2a$, the unstable behaviour is promoted if the weakening parameter $\beta = a\alpha > \beta_0$. In the following, we consider that this condition is always satisfied. The goal is now to compute the dynamic positive eigenvalues associated with the unstable behaviour. We focus here on the dependence of the positive eigenvalues $\{\lambda_i\}_{i=1,n}$ on the weakening parameter β. The curves $\lambda_0 = \Lambda_0(\beta)$, $\lambda_1 = \Lambda_1(\beta)$ and $\lambda_2 = \Lambda_2(\beta)$ are presented in Fig. 3. As expected, the number of positive eigenvalues depends on the value of β. When $\beta < \beta_0$, there is no positive eigenvalue. We have seen that in such a case, the fault is stable. When $\beta_0 < \beta < \beta_1$, we have only one positive eigenvalue and so on. λ_0^2, the largest positive dynamic eigenvalue plays a significant role in the unstable behaviour. It is associated with the eigenfunction $\Phi_0(x, y)$ that corresponds to the fundamental mode of deformation of the system. The curve $\lambda_0 = \Lambda_0(\beta)$ is monotonically increasing. This means that large values of β lead to very unstable behaviour. The asymptotic behaviour of the function Λ_0 when $\beta \to +\infty$ is $\lambda_0 = \beta$, also obtained for an infinite fault. For high weakening rate, a finite
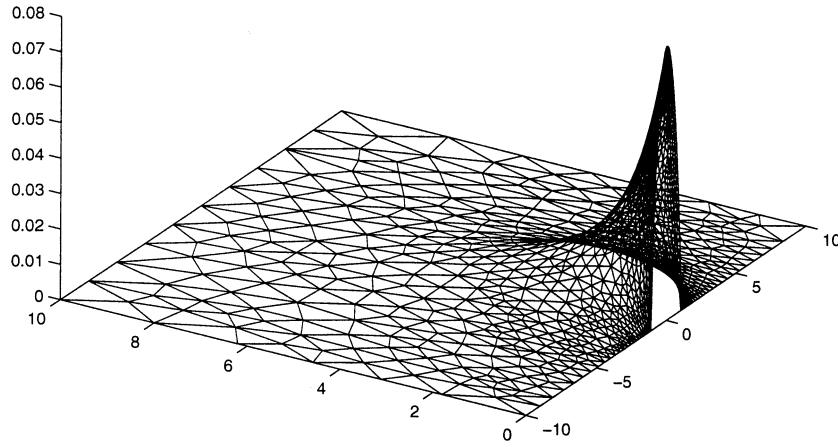
Figure 2. The first nondimensional static eigenfunction $\varphi_0(x, y)$. The maximum is located at the centre of the fault. The distribution of φ_0 on the fault is in good agreement with the slip distribution obtained by FDM. We note the rapid decay of φ_0 with x_2 the perpendicular coordinate.

fault behaves like an infinite fault. That is, the fault finiteness is not important in the qualitative behaviour of the system. Eq. (4) leads to:

$$l_c = \frac{a\pi}{\beta} \tag{35}$$

Consequently, we have:

$$\lim_{\beta \to \infty} l_c = 0 \tag{36}$$

Practically, when β is sufficiently high, we have $l_c \ll a$. A 'free' initiation process is possible, like on an infinite fault. The same qualitative behaviour would be expected if α was kept constant and $a \to +\infty$. When a is large enough, the relation $l_c \ll a$ is also satisfied, and the finite fault behaves like a infinite fault.

4.2 Accuracy of the spectral approach

In the previous section, we focused on λ_0^2, the largest positive eigenvalue. The underlying idea is that λ_0^2 and $\Phi_0(x, y)$ are
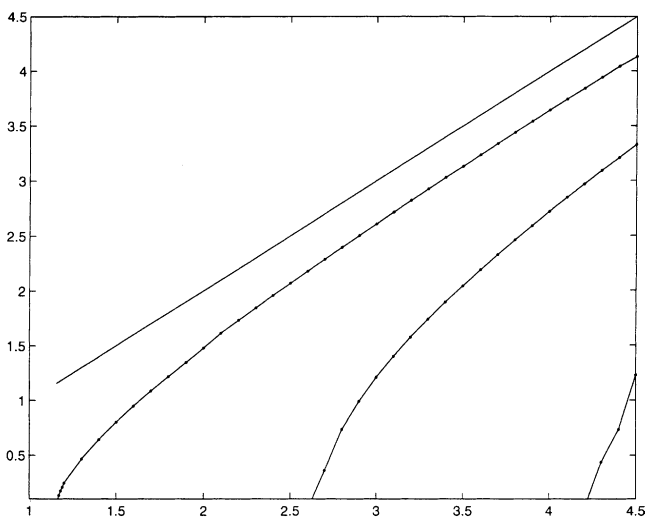

Figure 3. The functions $\lambda_0 = \Lambda_0(\beta)$, $\lambda_1 = \Lambda_1(\beta)$, $\lambda_2 = \Lambda_2(\beta)$ and the asymptote $\lambda = \beta$. Note that positive eigenvalues are reached when $\beta > \beta_0$. The static eigenvalues β_i can be seen in connection with the dynamic spectral problem. The β_i are defined as it follows: $\{\beta_i/\Lambda_i(\beta_i)=0\}$.

associated with the dominant part of the unstable evolution. The question is to know whether this assumption is correct, or not. To clear this point, we compute the slip rate evolution on a finite fault, either with a finite difference method or a finite element method. We consider a linear slip dependent friction :

$$\mu(u) = \max\left\{ \mu_s - \frac{\mu_s - \mu_d}{L_c} u, \mu_d \right\}$$

where u is the slip, μ_s and μ_d the friction coefficients and L_c the critical slip. We take $\mu_s = 0.8$, $\mu_d = 0.72$, $L_c = 0.17$ m. The weakening rate α is given by eq. (2). $S = \rho g z$ is the normal stress computed at a depth of 5000 m, and $G = \rho c^2$ is the rigidity modulus. The fault half length a is 500 m. We finally get: $\beta = a\alpha = 1.3$. According to Dascalu *et al.* (2000), we expect only one positive eigenvalue λ_0. Fig. (4a) presents the slip rate evolution on a finite fault, computed by a finite difference method over a period of 2 s. The initial perturbation propagates on the fault. After a few reflections, another process appears. This is the development of the unstable behaviour, characterized by an exponential growth with time. Fig. (4b) presents the same slip rate evolution, computed with the finite element spectral method. The agreement between the two methods is good. The main difference is that the dominant part, characterized by $(\lambda_0^2, \Phi_0(x, y))$ does not take into account the propagative part of the solution. However, the dominant part gives a correct description of the slip rate distribution. We can conclude that the dominant part represents essentially the unstable behaviour of the fault, and that the assumption that we made is correct. The finite element method allows to investigate the fault behaviour when $\beta \to \beta_0$, that is when $\lambda_0 \to 0$. For these values, long initiation duration are expected. Fig. (5) presents the slip evolution on a finite fault with a weakening parameter $\beta = \beta_0 + \varepsilon$. The computation gives $\lambda_0 = 5.10^{-4}$. The corresponding critical time (initiation duration) is $T_c = 2000$ s. For such a value of T_c, the finite difference method is inefficient. The slip evolution is so slow that numerical noise dominates over the initiation process. The model and the numerical method that we present here is able to produce long initiation duration (more than 30 minutes in this example). The spectral analysis that we propose is valid for any $\lambda_0 > 0$, even for really small values close to zero. So it is theoretically possible to produce a very broad range of initiation duration, even with this extremely simple model of a finite fault with linear friction.
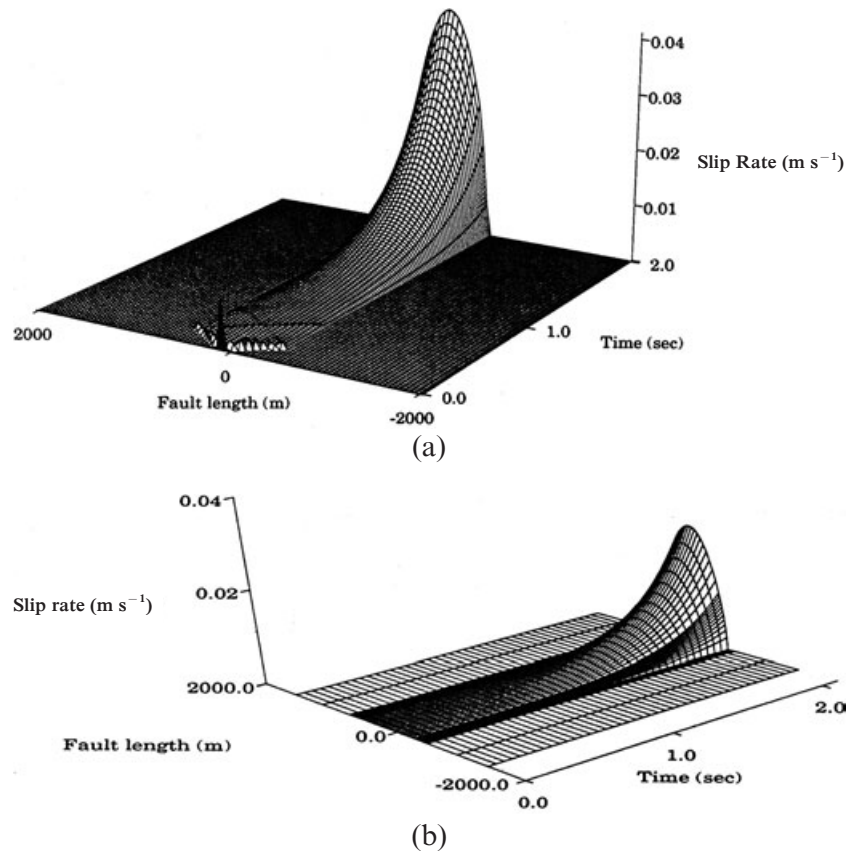
(a)

(b)

Figure 4. Comparison of the finite difference (a) and the finite element (b) methods. The parameters are given in the text. We note that the dominant part $w_d(t, x, y)$ provides a correct description of the unstable evolution of the slip.

5 FAULT INTERACTION

Up to now, we have considered only a simple homogeneous fault. However, it is obvious that faults are heterogeneous, composed of segments that may or may not interact. This last point is of importance in earthquake studies. The interaction of fault segments is a key issue in the prediction of the highest possible magnitude of the next event. In this section, we study the possible interaction of fault segments during the initiation process. This problem is completely different from the possible interaction of fault segments during the propagation of the rupture front.
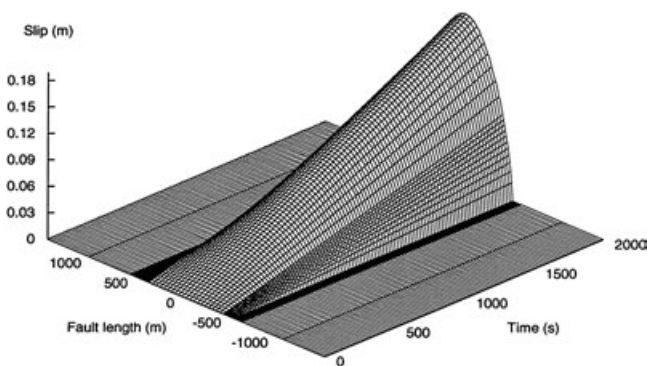

Figure 5. The unstable behaviour of the slip evolution may take time to develop as $\lambda_0 \to 0$. In this example, the critical time T_c is about 2000 seconds. The beginning of the slip velocity evolution is so slow that it is often qualified of 'quasistatic' growth.

5.1 Interaction of two fault segments

We consider here the case of a fault zone composed of two identical frictional segments (each of length $2a$) separated by a rigid barrier of variable size. The goal is to show the reality of the interaction between the two segments during the eventual initiation process. We use the numerical approach already described to investigate the behaviour of the fault system. The distance between the two segments is variable. We solve the static spectral problem and compute the value of β_0 for different spacing between the segments. The results are presented in Fig. (6). As physically expected, the constant β_0 for the system decreases as the distance between the two segments decreases, which proves the interaction between the two segments. On the contrary, when the distance between the segments increases, β_0 also increases up to the constant of stability of an homogeneous fault. That is the two segments do not interact anymore. The maximum distance of interaction is of the order of $10a$, where a is the half length of a segment.

5.2 The case of an heterogeneous fault

We consider a fault composed of several (11) segments, all identical, with the same weakening rate β_{local}, separated by rigid barriers. We aim to show that the dynamic behaviour of this complex fault system is equivalent to the dynamic behaviour of a simple homogeneous fault with a weakening rate $\beta_{equivalent}$. The static spectral problem associated to this complex geometry

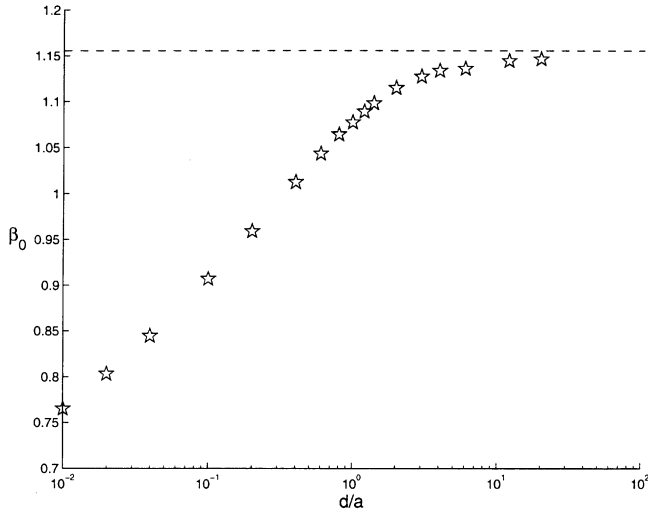**Figure 6.** Interaction of two fault segments. Two identical fault segments (of length 2a) are distant from d, variable. The constant of stability β_0 of the system is computed. Note the decreasing of β_0 as d decreases. The distance of interaction is of the order of 10a. Over this distance, the universal constant of stability is nearly constant and equals the constant of stability of one fault segment (dashed line).

is solved. We get $\beta_0 = 10.3$. The weakening parameter of each individual segment has to be greater than β_0 to promote the unstable behaviour of the fault system. We choose $\beta_{local} = 13.08$. Then, the dynamic spectral problem is solved for this particular geometry.

Fig. (7) presents the first dynamic eigenfunction Φ_0^h corresponding to the heterogeneous fault system. This eigenfunction has to be compared to φ_0, computed for one fault segment and presented in Fig. (2). At the first glance, these two functions look very similar. However, Φ_0^h is highly heterogeneous in the close vicinity of the fault. On the other hand, the global shape (envelope) is similar to φ_0, which seems to indicate that the heterogeneous system behaves like an homogeneous one. The largest eigenvalue is computed to be $\lambda_0^h \approx 4.6$ and is associated with Φ_0^h. With the help of the curve $\lambda_0 = \Lambda_0(\beta)$ (defined for one homogeneous fault segment) presented in Fig. (3), it is possible to derive the value of the corresponding weakening parameter:

$$\beta = \Lambda_0^{-1}(\lambda_0^h)$$

A homogeneous fault with such a weakening rate will lead to $\lambda_0 = \lambda_0^h$. We argue that this particular value of β is the
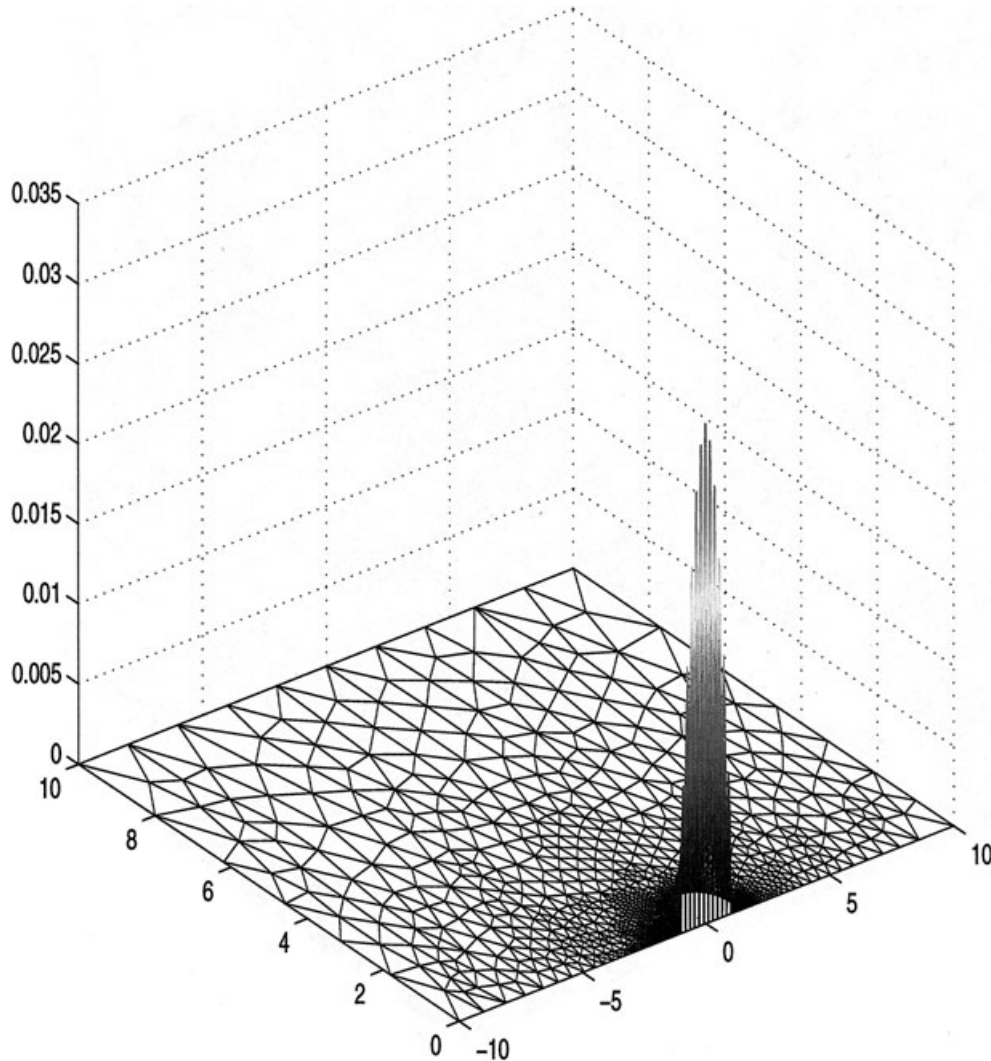

Figure 7. First dynamic eigenfunction Φ_0^h of the heterogeneous fault system.

equivalent weakening rate. That is:

$$\beta_{\text{equivalent}} = \Lambda_0^{-1}(\lambda_0^h) \tag{37}$$

This last hypothesis will be discussed in next section.

6 THE INITIATION PATTERN: A POSSIBLE SIGNATURE OF INSTABILITY

6.1 Case of one homogeneous fault

Characterizing the unstable behaviour of a fault will be a step in earthquake prediction. Through eq. (1) we have seen the simple dependency of the dominant part of the unstable slip evolution with respect to the y coordinate in the case of an infinite fault. This can be presented as follows

$$-\frac{\partial_y w^d(t, x, y)}{w^d(t, x, y)} = \alpha, \quad \text{everywhere in} \quad R \times R_+, \tag{38}$$

i.e. during the initiation phase the linear weakening condition on the fault is transmitted everywhere in the interior of the elastic medium. This property can be a candidate for the signature of the instable evolution of the finite fault model. The question is how to find a similar property in case of a finite fault. Let us suppose that we deal with a slow initiation

(i.e. $N = 1$, $\lambda_1^2 < 0 < \lambda_0^2 \ll 1$) or we can neglect the contribution of all the other eigenfunctions with respect to the first one (i.e. $0 < \lambda_{N-1}^2 < \ldots < \lambda_1^2 \ll \lambda_0^2$). In this case

$$w^d(t, x_1, x_2)$$

$$\approx \left[\cosh(c|\lambda_0|t/a) W_0^0 + a \frac{\sinh(c|\lambda_0|t/a)}{c|\lambda_n|} W_0^1 \right] \Phi_0(x_1, x_2),$$

and the associated ratio given by eq. (38) can be deduced as:

$$B_\beta(x_1, x_2) = -\frac{\partial_{x_2} \Phi_0(x_1, x_2)}{\Phi_0(x_1, x_2)}, \tag{39}$$

This ratio represents the information about the weakening rate of the fault, when it is defined. Actually, B_β is defined everywhere on $\Omega - \Gamma_d$. On Γ_c ($x_2 = 0$) we have the relation $B_\beta = \beta$. Fig. (8) presents the function $B_{\beta_0}(x_1, x_2)$ computed in the static case. We have focused on the behaviour of B_{β_0} close to the fault Γ_c. The minimum value of the function is β_0. It is reached on the fault and on a small domain close to the fault. Note the typical shape of the function, organized in a band of the size of the fault length. Fig. (9) presents some computations for different weakening rates β for 1.2–5. The general shape of B_β is the same for all β and then defines an initiation pattern that qualitatively characterizes the unstable behaviour of the fault. The most interesting point is the existence of a domain of B_β over which $B_\beta(x, y) = \beta$. This signifies that the weakening parameter can be measured in the surrounding elastic body. We can define now the domain of confidence as the part of the
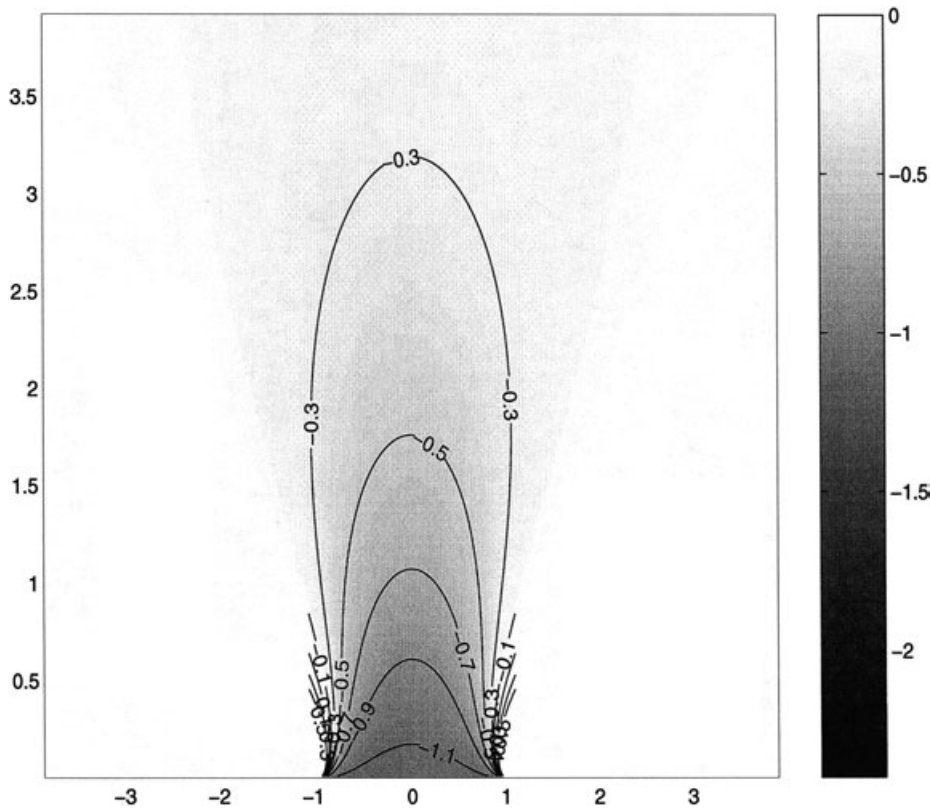

Figure 8. Map view of the function $B_{\beta_0}(x_1, x_2)$. Note the typical shape of the function in the vicinity of the fault surface Γ_f (emphasized by the black lines). Note also that the minimum of the function is β_0 and that this minimum is reached on Γ_f and on a small domain close to the fault.
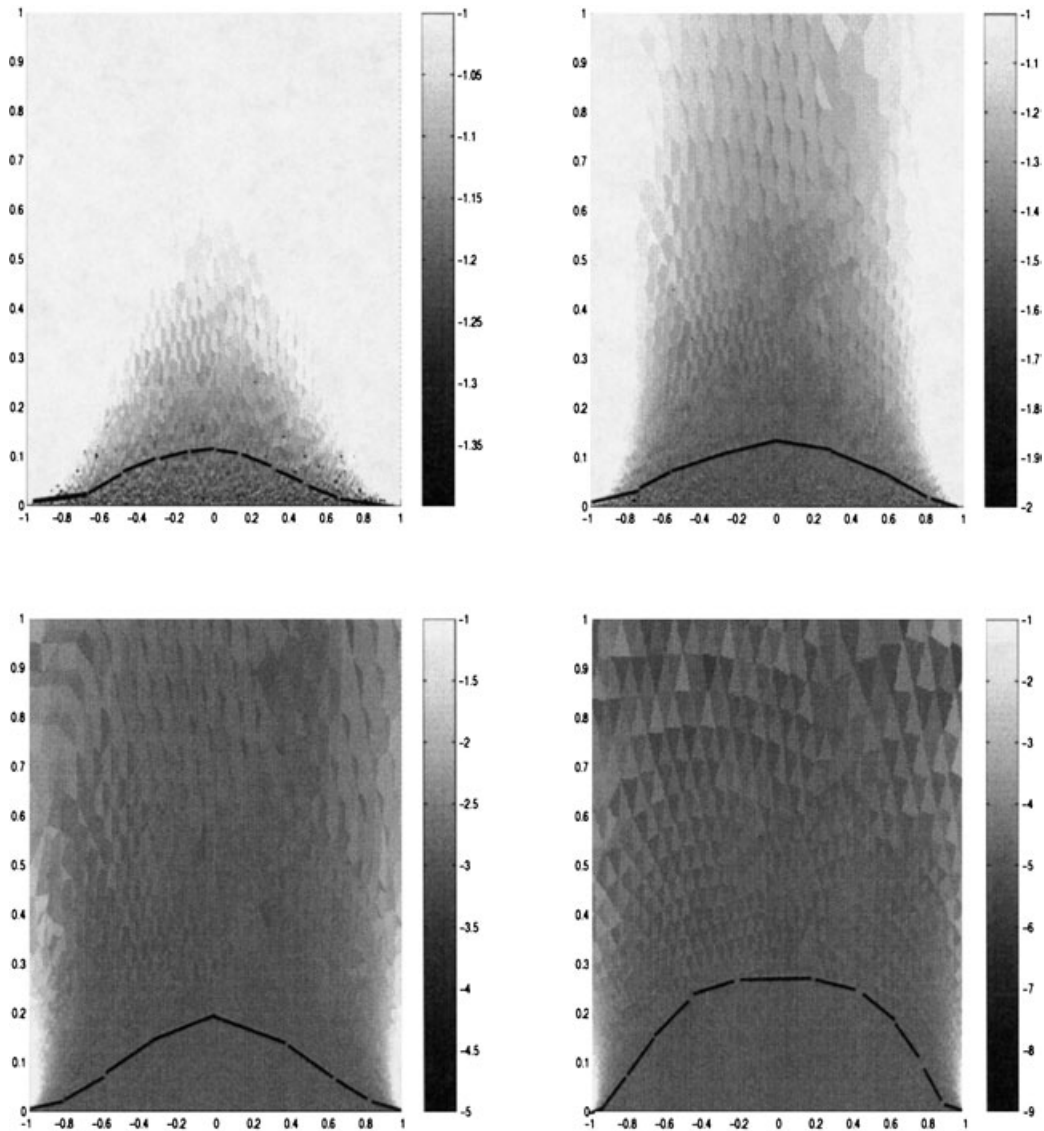
Figure 9. Map view of the $B_\beta(x_1, x_2)$ in the vicinity of the fault for different values of the weakening parameter. From left to right and top to bottom: $\beta = 1.2, 1.5, 3, 5$. Note the same shape of the function in the four different cases. The black line emphasizes the limit of the domain of confidence over which the function is nearly constant and equals β. The size of this domain is an increasing function of β.

elastic body where the previous property is satisfied:

$$D_c(\beta) = \{(x_1, x_2); B_\beta(x_1, x_2) = \beta\} \tag{40}$$

The fault surface Γ_f is always included in D_c. The extension of the domain of confidence is an increasing function of the weakening rate β. From the relation between λ_0 and β (see Fig. 3) and the measure of β over the domain of confidence, it is possible to get the largest positive eigenvalue. Since the initiation duration is inversely proportional to λ_0, we are able to prescribe a critical time, that is we can predict the time of occurrence of the future event.

6.2 Case of an heterogeneous fault

We consider the case of a fault zone composed of eleven identical frictional segments (described in Section 5.2). We now compute the function $B_\beta(x_1, x_2)$ for this complex fault system.

The result is presented in Fig. (10). As already seen, close to each individual fault segment, an initiation pattern develops in the elastic medium, associated with a local domain of confidence over which β_{local} can be measured. The striking feature of Fig. (10) is the existence of a wide domain over which $B_\beta(x_1, x_2)$ is nearly constant, independent from the individual fault segments but closely related to the whole fault system. All over this domain, we have the following relation:

$$-\frac{\partial_{x_2} \Phi_0(x_1, x_2)}{\Phi_0(x_1, x_2)} = \beta_{equivalent}$$

That is, all over this wide domain, it is possible to measure the collective behaviour of all the fault segments, similar to the behaviour of an homogeneous fault with $\beta = \beta_{equivalent}$. Some strong results arise from these computations:

(i) An initiation pattern develops inside the elastic medium and is characteristic of the unstable behaviour of the fault system.
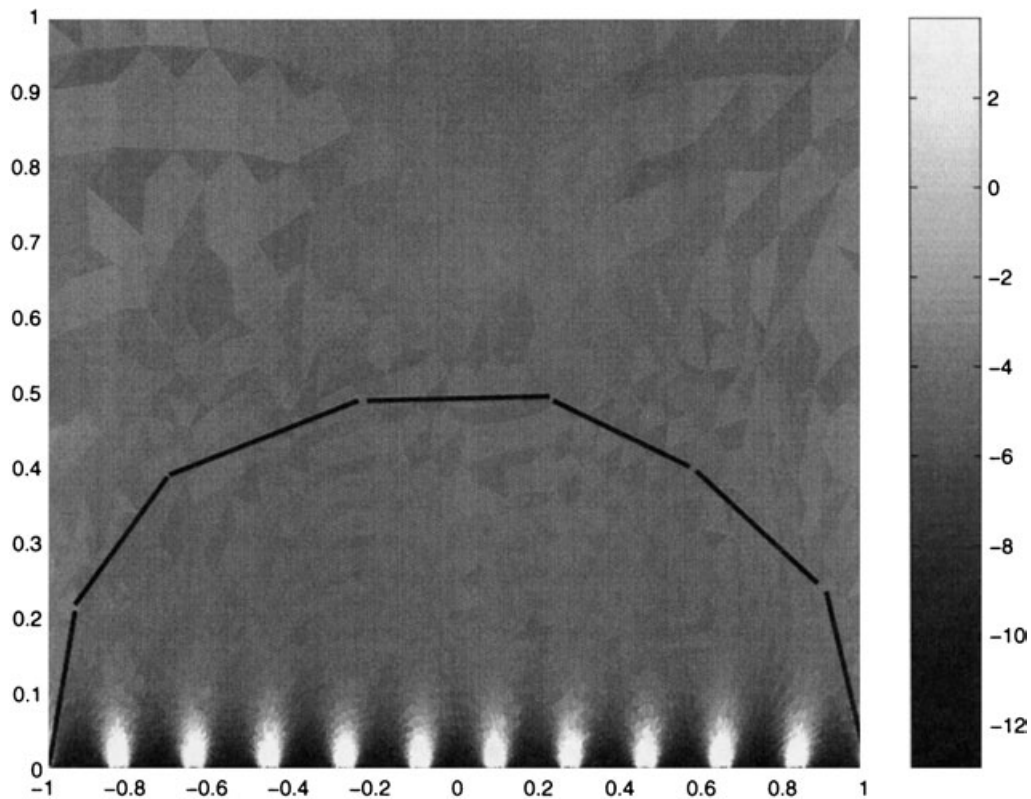
Figure 10. Map view of the function $B_\beta(x_1, x_2)$ in the vicinity of the fault zone, composed of 11 interacting fault segments. Note the local initiation pattern associated with each of the fault segment, and also the global initiation pattern. The black line limits the global domain of confidence associated with the unstable behaviour of the whole fault system. All over this domain, the function $B_\beta(x_1, x_2) \approx \beta_{\text{equivalent}}$.

(ii) The collective behaviour of all the segments is transmitted in the medium and can be measured over a wide domain.

(iii) There is a spectral equivalence between a complex heterogeneous fault (β_{local}, λ_0^h, Φ_0^h) and an homogeneous fault ($\beta_{\text{equivalent}} = \Lambda_0^{-1}(\lambda_0^h)$, $\lambda_0 = \lambda_0^h$, Φ_0).

These results are in perfect compliance with those of Campillo *et al.* (2001), who used finite difference time domain computations to demonstrate the accuracy of an effective friction law deduced from the properties of the strain field inside the elastic body.

7 DISCUSSION

The unstable behaviour of a fault is successfully modelled by the dominant part of the slip rate evolution. The model that we develop in this paper is rather simple: a finite homogeneous fault under a linear slip dependent friction law, characterized by the weakening rate α and its half length a through the parameter $\beta = a\alpha$. This model produces long initiation duration, up to at least 30 minutes, as presented in Fig. (5). Many other processes may be involved in the initiation process over such a long period of time. We do not argue that these physical mechanisms, such as fluids effects, are not important, we just show that a simple fault model can produce a very broad range of initiation durations with no need for other mechanisms.

We have shown that the analysis we performed on a finite homogeneous fault remains valid for a heterogeneous fault. The collective behaviour of interacting fault segments is very similar to the homogeneous finite fault behaviour. The equivalent weakening rate is given by the relation $\lambda_0 = \Lambda_0(\beta)$. The equivalence is complete in terms of initiation process, that is λ_0 is the same for the two faults. Therefore, the critical time (the initiation duration) is the same in both cases. The equivalent homogeneous fault is a sort of homogenization of the complex fault. This technique may be used for different scales of heterogeneity to provide a correct description of the global behaviour of complex, highly heterogeneous fault systems. However, the homogenization implicates the loss of information on how the rupture process will develop in detail. The rupture complexity observed both in laboratory experiments or in strong motion inversions will be lost by these homogenization techniques.

The transmission of information about the weakening rate the elastic medium offers the possibility to constrain the time of occurrence of the next event, even without knowing anything on the fault. The existence of an initiation pattern associated with the unstable behaviour of the fault and the measure of the function $B_\beta(x, y)$ is sufficient to give a good approximation of λ_0, and therefore to prescribe the critical time. However interesting these results may be, they have to be confirmed by other methods, and moreover they have to be extended to the 3D case. Many other parameters have to be taken in account, such as the fault geometry or the orientation of the fault plane. This study appears like a first attempt to recognize and characterize a possible signature of the unstable behaviour of a fault, that is an initiation pattern.

8 CONCLUSIONS

We presented a numerical method based on the finite elements techniques to study the problem of the initiation process on a finite fault. This method allows accurate computations for large eigenvalues which is not the case for the numerical approach based on the integral equations proposed by Dascalu *et al.* (2000). In case of an unstable fault, we show that the catastrophic evolution of the slip rate is successfully modelled by the dominant part, formed by the contributions of the positive eigenvalues. We give the relation $\lambda_0 = \Lambda_0(\beta)$ between the weakening rate β and the largest positive eigenvalue λ_0 that largely controls the unstable behaviour. We show that some information about the weakening rate β is transmitted in the elastic medium over a domain of confidence. We present the initiation pattern associated with the unstable behaviour. This analysis remains valid for more complex fault systems. We show the complete equivalence, in terms of initiation process, between a heterogeneous fault characterized by $(\beta_{\mathrm{local}}, \lambda_0^h, \Phi_0^h)$ and a homogeneous fault characterized by $(\beta_{\mathrm{equivalent}}, \lambda_0^h, \Phi_0)$ where $\beta_{\mathrm{equivalent}} = \Lambda_0^{-1}(\lambda_0^h)$. These preliminary results have to be confirmed by other methods, and moreover, they have to be extended to the 3D case.

ACKNOWLEDGMENTS

REFERENCES

Campillo, M. & Ionescu, I.R., 1997. Initiation of antiplane shear instability under slip-dependent friction, *J. geophys. Res.,* **102,** 20 363–20 371.

Campillo, M., Favreau, P., Ionescu, I.R. & Voisin, C., 2001. On the effective friction law of an heterogeneous fault, *J. geophys. Res.,* **106,** 16 307–16 322.

Dascalu, C., Ionescu, I.R. & Campillo, M., 2000. Fault finiteness and initiation of dynamic shear instability, *Earth planet. Sci. Lett.,* **177,** 163–176.

Dieterich, J.H., 1979. Modeling of rock friction 1. Experimental results and consitutive equations, *J. geophys. Res.,* **84,** 2161–2175.

Ida, Y., 1972. Cohesive force along the tip of a longitudinal shear crack and Griffith's specific surface theory, *J. geophys. Res.,* **77,** 3796–3805.

Ionescu, I.R. & Campillo, M., 1999. The influence of the shape of the friction law and fault finiteness on the duration of initiation, *J. geophys. Res.,* **104,** 3013–3024.

Knopoff, L., Landoni, J.A. & Abinante, M.S., 2000. Causality constraint for fractures with linear slip weakening, *J. geophys. Res.,* **105,** 28 035–28 044.

Ohnaka, M., Kuwahara, Y. & Yamamoto, K., 1987. Constitutive relations between dynamic physical parameters near a tip of the propagating slip zone during stick slip shear failure, *Tectonophysics,* **144,** 109–125.

Ohnaka, M. & Kuwahara, Y., 1990. Characteristic features of local breakdown near a crack-tip in the transition zone from nucleation to unstable rupture during stick-slip shear failure, *Tectonophysics,* **175,** 197–220.